



This is the accepted manuscript made available via CHORUS. The article has been published as:

# Muonic bound systems, virtual particles, and proton radius

U. D. Jentschura

Phys. Rev. A **92**, 012123 — Published 27 July 2015

DOI: [10.1103/PhysRevA.92.012123](https://doi.org/10.1103/PhysRevA.92.012123)

# Muonic Bound Systems, Virtual Particles and Proton Radius

U. D. Jentschura

*Department of Physics, Missouri University of Science and Technology, Rolla, Missouri 65409, USA*

The proton radius puzzle questions the self-consistency of theory and experiment in light muonic and electronic bound systems. Here, we summarize the current status of “new virtual particle” models as well as Lorentz-violating models which have been proposed in order to explain the discrepancy. Highly charged one-electron ions and muonic bound systems have been used as probes of the strongest electromagnetic fields achievable in the laboratory. The average electric field seen by a muon orbiting a proton is comparable to hydrogenlike Uranium and, notably, larger than the electric field in the most advanced strong-laser facilities. Effective interactions due to virtual annihilation inside the proton (“lepton pairs”) and process-dependent corrections (nonresonant effects) are discussed as possible explanations of the proton size puzzle. The need for more experimental data on related transitions is emphasized.

PACS numbers: 12.20.Ds, 11.25.Tq, 11.15.Bt

## I. INTRODUCTION

Recent muonic hydrogen experiments [1, 2] have resulted in the most severe discrepancy of the predictions of quantum electrodynamics with experiment recorded over the last few decades. In short, both (electronic, atomic) hydrogen experiments (for an overview see Ref. [3]) as well as recent scattering experiments lead to a proton charge radius of about  $\langle r_p \rangle \approx 0.88$  fm, while the muonic hydrogen experiments [1, 2] favor a proton charge radius of about  $\langle r_p \rangle \approx 0.84$  fm.

Few-body bound electronic and muonic systems belong to the most intensely studied fundamental physical entities; a combination of atomic physics and field-theoretical techniques is canonically employed [4–14]. Here, we aim to discuss conceivable explanations for the discrepancy and highlight a few aspects which set the muonic systems apart from any other bound states which have been studied spectroscopically so far. To this end, in Sec. II, we briefly summarize the status of “virtual particle” models discussed in the literature and supplement previous approaches with a discussion of the role of axion terms which might be significant in the strong magnetic fields used in the muonic hydrogen experiments. In Sec. III, we show that muonic hydrogen (as well as muonic hydrogen-like ions with low nuclear charge number  $Z$ ) constitute some of the most sensitive probes of high-field physics to date; concomitant speculations about novel phenomena in the strong fields inside the proton are discussed. Finally, a possible role of process-dependent corrections in experiments is mentioned in Sec. IV. Conclusions are reserved for Sec. V. We use SI mksA units unless indicated otherwise.

## II. VIRTUAL PARTICLES AND MUONIC HYDROGEN

From the point of view of quantum field theory, the most straightforward explanation for the proton radius puzzle in muonic hydrogen would involve a “subversive”

virtual particle that modifies the muon-proton interaction at distances commensurate with the Bohr radius of muonic hydrogen,

$$a_\mu = \frac{\hbar}{\alpha_{\text{QED}} m_r c} = 2.84708 \times 10^{-13} \text{ m}, \quad (1)$$

where  $\alpha_{\text{QED}}$  is the fine-structure constant, and  $m_r = m_\mu m_p / (m_\mu + m_p)$  is the reduced mass. The distance regime of  $a_\mu \approx 300$  fm is intermediate between the Bohr radius of (ordinary) hydrogen and the proton radius.

In consequence, the possible role of millicharged particles, which modify the Coulomb force law in this distance regime, has been analyzed in Ref. [13]. These particles could conceivably modify the photon propagator at energy scales  $\hbar c/a_\mu$  via vacuum-polarization insertions into the photon line. Supplementing this analysis, in Ref. [12], conceivable hidden (massive) photons have been analyzed. Particles with scalar and pseudo-scalar couplings have been the subject of Ref. [15]. A model which explicitly breaks electron-muon universality, introducing a coupling of the right-handed muonic fermion sector to a  $U(1)$  gauge boson, has been investigated in Ref. [16]. One should notice, though, that the explicit breaking of the universality according to Eq. (7) of Ref. [16] appears as somewhat artificial. The reduction in the muonic helium nuclear radius by  $\Delta r_{\text{He}}^2 = -0.06 \text{ fm}^2$  as predicted by the model proposed in Ref. [16] has the opposite sign as compared to the results of the experiments [17, 18], that were carried out about four decades ago and roughly observe a 4% *lower* cross section for muons scattering off of protons as opposed to electrons being scattered off the same target.

Likewise, in a recent paper on Lorentz-violating terms in effective Dirac equations [19], the authors assume an explicit breaking of electron-muon universality (see Sec. IIC3 of Ref. [19], remark in the lower right-hand column), where the authors explicitly state that they assume only muon-sector Lorentz violation, so that effects arise in  $H_\mu$  spectroscopy but are absent in H spectroscopy and electron elastic scattering. *Cum grano salis*, this assumption appears to be a little artificial because it would

modify the effective Dirac equation for muons as compared to that of electrons. In general, Lorentz-violating parameters may break rotational invariance, and thus have an effect on the  $S$ - $P$  transitions measured in [1, 2] [see the derivation in Eqs. (21)–(25) of Ref. [19]].

In the virtual particle models from Refs. [13, 15, 16], it has been found necessary to fine-tune the coupling constants in order to avoid conflicts with muon and electron  $g - 2$  measurements, which otherwise provide constraints on the size of the “new physics terms” due to their relatively good agreement with experiment (for a discussion, see Ref. [13]). Furthermore, attempts to reconcile the difference based on higher moments of the proton charge distribution (its “higher-order shape”, see Ref. [20]) face difficulty when confronted with scattering experiments which set relatively tight constraints on the higher-order corrections to the proton’s shape.

One class of models which have not been explored hitherto concern electrodynamics with axion-like particles (ALPs, see Refs. [21–24]). In the experiments [1, 2], strong magnetic fields on the order of about 5 T are used to collimate the muon beam. Axion terms could potentially influence the results of the spectroscopic measurements. We start from the Lagrangian [25–29] for a pseudoscalar ( $0^-$ ) axion-like particle (temporarily setting  $\hbar = c = \epsilon_0 = 1$ )

$$\begin{aligned}\mathcal{L} = & -\frac{1}{4}F^{\mu\nu}F_{\mu\nu} - \frac{g}{4}\phi\tilde{F}^{\mu\nu}F_{\mu\nu} \\ & + \frac{1}{2}\partial_\mu\phi\partial^\mu\phi - \frac{1}{2}m_\phi^2\phi \\ = & \frac{1}{2}(\vec{E}^2 - \vec{B}^2) + g\phi\vec{E}\cdot\vec{B} \\ & + \frac{1}{2}\partial_\mu\phi\partial^\mu\phi - \frac{1}{2}m_\phi^2\phi.\end{aligned}\quad (2)$$

Here, according to Ref. [29], the axion’s two-photon coupling constant reads as

$$g \equiv G_{A\gamma\gamma} = \frac{\alpha_{\text{QED}}}{2\pi f_A} \left( \frac{E}{N} - \frac{2}{3} \frac{4+z}{1+z} \right) \quad (3)$$

( $\phi$  is the axion field,  $m_\phi$  is the axion mass,  $m_\phi f_A \approx m_\pi f_\pi$  where  $f_\pi$  is the pion decay constant and  $m_\pi$  the pion mass, while  $z = m_u/m_d$  is the quark mass ratio). Grand unified models [30–34] assign rational fractions to the ratio  $E/N$  of the electromagnetic to the color anomaly of the axial current associated with the axion. Possible values are  $E/N = 8/3$  (see Refs. [30, 31]) or zero [32, 33]. In Eq. (2), the electromagnetic field strength tensor  $F_{\alpha\beta}$  and its dual  $\tilde{F}_{\alpha\beta}$  have their usual meaning.

It is interesting to consider the leading correction to the Coulomb potential in strong magnetic fields, on the order of 5 T, due to the axion-photon conversion amplitude inherent to the Lagrangian (2) (see Figs. 1 and 2). We shall first assume that the vacuum expectation value of the axion field vanishes [35, 36] and consider the tree-level correction to the Coulomb potential given in Fig. 2.

We match the scattering amplitude according to Chap. 83 of Ref. [37] (see also [38]) and calculate the potential, generated by the axion-like particle, due to the diagram in Fig. 2. The pseudoscalar axion-like particle (ALP) potential is given as

$$\begin{aligned}V_{\text{ALP } 0^-}(\vec{k}) &= (\vec{k} \cdot \vec{B})^2 \frac{4\pi Z\alpha g^2}{\vec{k}^4(\vec{k}^2 + m_\phi^2)} = (\vec{k} \cdot \vec{B})^2 f(\vec{k}), \\ f(\vec{k}) &= \frac{4\pi Z\alpha g^2}{\vec{k}^4(\vec{k}^2 + m_\phi^2)}.\end{aligned}\quad (4)$$

In coordinate space, we therefore have

$$\begin{aligned}V_{\text{ALP } 0^-}(\vec{r}) &= -(\vec{B} \cdot \vec{\nabla})^2 f(\vec{r}), \\ f(\vec{r}) &= 4\pi Z\alpha g^2 \left( \frac{e^{-m_\phi r} - 1}{4\pi m_\phi^4 r} - \frac{r}{8\pi m_\phi^2} \right).\end{aligned}\quad (5)$$

With  $f(\vec{r}) = f(r)$ , we have the second derivative as

$$(\vec{B} \cdot \vec{\nabla})^2 f(r) = \left( \frac{\vec{B}^2}{r} - \frac{(\vec{B} \cdot \vec{r})^2}{r^3} \right) f'(r) + \frac{(\vec{B} \cdot \vec{r})^2}{r^2} f''(r). \quad (6)$$

Differentiating and expanding for small  $m_\phi$ , one obtains

$$\begin{aligned}V_{\text{ALP } 0^-}(\vec{r}) &= Z\alpha g^2 \left( \frac{\vec{B}^2}{3m_\phi} - \frac{\vec{B}^2 \vec{r}^2 + (\vec{B} \cdot \vec{r})^2}{8r} \right) \\ &\sim -\frac{Z\alpha g^2}{8r} (\vec{B}^2 \vec{r}^2 + (\vec{B} \cdot \vec{r})^2)\end{aligned}\quad (7)$$

where we subtract the constant shift. This effective potential is independent of the ALP mass  $m_\phi$  provided  $m_\phi$  is much smaller than other mass scales in the problems, such as  $m_e$  and  $m_\mu$  (see also Fig. 3). The  $1S$  expectation value is

$$\begin{aligned}\delta E &= \left\langle 1S \left| -\frac{Z\alpha g^2}{8r} (\vec{B}^2 \vec{r}^2 + (\vec{B} \cdot \vec{r})^2) \right| 1S \right\rangle \\ &= -\frac{g^2 \vec{B}^2}{4m_r} = -\epsilon_0 (\hbar c)^3 \frac{g^2 \vec{B}^2}{4m_r},\end{aligned}\quad (8)$$

where  $m_r$  is the reduced mass of the bound system, and SI mksA units are restored in the last step. Otherwise, according to Table 5 of Ref. [27], we have

$$g < 4.9 \times 10^{-7} \text{ GeV}, \quad m_\phi \lesssim 0.5 \text{ meV}. \quad (9)$$

For the parameters  $|\vec{B}| = 5 \text{ T}$  and  $g = 5 \times 10^{-7} \text{ GeV}^{-1}$ , we obtain

$$\delta E_H = -1.67 \times 10^{-31} \text{ eV}, \quad \delta E_{\mu H} = -6.28 \times 10^{-34} \text{ eV}. \quad (10)$$

The smallness of these results excludes ALPs as possible explanations for the proton radius puzzle. A possible scenario with a nonvanishing vacuum expectation value of the axion field (see also Ref. [39, 40]) is studied in Appendix A.

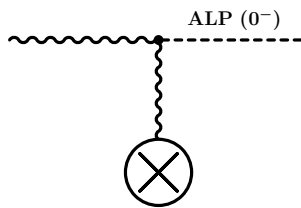


FIG. 1: ALP-photon conversion in a strong magnetic field according to the interaction term in the Lagrangian given in Eq. (2). The large encircled cross denotes the interaction with an external magnetic field.

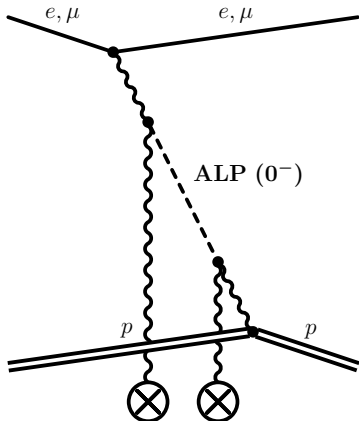


FIG. 2: The leading (tree-level) correction to the Coulomb potential due to the ALP-photon interaction is given by the tree-level diagram shown. The upper fermion line corresponds to an electron ( $e$ , ordinary hydrogen) or a muon ( $\mu$ , muonic hydrogen).

### III. STRONG-FIELD ELECTRODYNAMICS

Muonic bound systems have been used as probes of the strongest electromagnetic fields since the 1970s (see Ref. [5]), but progress has eventually been hindered due to electron screening [41]. Typically, transitions in high- $Z$  muonic ions involve highly excited, non- $S$  states [42–44], where the average field seen by the orbiting electron is reduced due to the higher principle quantum number. In view of the current muonic hydrogen discrepancy, it is useful to recall just how strong these fields are, especially in very simple bound systems, where shielding electrons are absent [45, 46]. The conceivable presence of “novel phenomena” in the very strong electromagnetic fields within highly charged ions has been mentioned as a significant motivation for the study of these systems [7, 8, 47, 48]. According to Eq. (2) of Ref. [7] and the more comprehensive discussion of Ref. [47], a conceivable nonlinear correction term (contact interaction) has been mentioned for high-field quantum electrodynamics. In view of this situation, it is indicated to compare the field strengths in highly charged (electronic) ions to those reached for low excited states in muonic hydrogen and

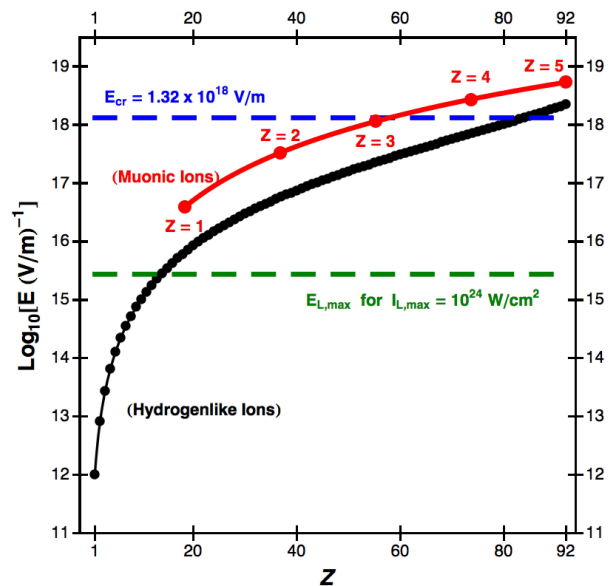


FIG. 3: (Color.) Plot of the average field strength (13a) experienced by a bound electron or muon in a one-muon ion (red line,  $1 \leq Z \leq 5$ ), and for hydrogenlike (electronic) ions in the range  $1 \leq Z \leq 92$ . For comparison, the average field strength in a laser field of intensity  $10^{24} \text{ W cm}^{-2}$  is given [49]. The Schwinger critical field strength is denoted as  $E_{\text{cr}}$ .

low- $Z$  muonic ions.

A measure for the strongest electromagnetic fields which can be described by perturbative electrodynamics is the Schwinger critical field strength [50–53]

$$E_{\text{cr}} = 1.32 \times 10^{18} \frac{\text{V}}{\text{m}}. \quad (11)$$

The electric field around the proton reaches the Schwinger critical field already at a distance  $0.116 a_\mu$  Bohr radii of the muonic hydrogen system, where  $a_\mu$  is given in Eq. (1). Let us consider bound one-muon ions in the region of low nuclear charge numbers  $1 \leq Z \leq 5$ . The probability of finding a  $1S$  muon inside the region of super-critical field strength, in one-muon ions of nuclear charge number  $1 \leq Z \leq 5$ , evaluates as follows,

$$p_{\text{cr}}(Z=1) = 0.17\%, \quad (12a)$$

$$p_{\text{cr}}(Z=2) = 1.18\%, \quad (12b)$$

$$p_{\text{cr}}(Z=3) = 3.36\%, \quad (12c)$$

$$p_{\text{cr}}(Z=4) = 6.73\%, \quad (12d)$$

$$p_{\text{cr}}(Z=5) = 11.2\%. \quad (12e)$$

The field scales as  $1/r^2$  for small distances. In Fig. 3, to supplement a corresponding investigation in Fig. 2 of Ref. [7], we investigate the electric field strength felt by a bound muon in a “muonic hydrogenlike” system (only one orbiting particle) in the region of low nuclear charge number. We start from the ground-state expectation value of the electric-field operator, which is obtained

as the gradient of the Coulomb potential. Within the non-relativistic approximation (we SI mksA units), the result reads as

$$\langle E \rangle = \left\langle 1S \left| \left( -\frac{\partial}{\partial r} \frac{Z|e|}{4\pi\epsilon_0 r} \right) \right| 1S \right\rangle = 2 Z^3 \frac{m_r^2}{m_e^2} \mathcal{E}_0, \quad (13a)$$

$$\mathcal{E}_0 = \frac{e \alpha_{\text{QED}}^2 m_e^2 c^2}{4\pi \epsilon_0 \hbar^2} = 5.14 \times 10^{11} \frac{\text{V}}{\text{m}}. \quad (13b)$$

Here,  $m_r$  is the reduced mass of the atomic system,  $m_e$  is the electron mass, and  $\mathcal{E}_0$  denotes the “standard” atomic field strength observed at one Bohr radius in the “standard” hydrogen atom (it is equal to the atomic unit of the electric field strength). The prefactor 2 in Eq. (13a) is a consequence of our taking the quantum mechanical expectation value as opposed to evaluating the classical expression at the (shifted) Bohr radius. For ultra-relativistic systems, Eq. (13a) is replaced by the expectation value of the fully relativistic Dirac–Coulomb wave function [54]; the relativistic correction factor amounts to the replacement

$$\langle E \rangle \mapsto \frac{\langle E \rangle}{2 - \sqrt{1 - (Z\alpha_{\text{QED}})^2} - 2(Z\alpha_{\text{QED}})^2}, \quad (14)$$

which does not change the order-of-magnitude of the result. The decisive factor in Eq. (13a) is the prefactor  $Z^3 (m_r/m_e)^2$ , which is responsible for an enhancement of the field strength by six orders of magnitude in the range  $1 \leq Z \leq 92$  for electronic system, but also for a considerable enhancement in muonic systems, where

$$\left( \frac{m_r}{m_e} \right)^2 \rightarrow \left( \frac{m_\mu m_p}{(m_\mu + m_p) m_e} \right)^2 \approx 3.45 \times 10^4. \quad (15)$$

For a one-muon ion, the average electric field strengths at  $Z = 4$  and  $Z = 5$  surpass the average electric field strength in hydrogenlike Uranium (see Fig. 3).

Furthermore, the average field strength felt by a bound  $1S$  electron in one-muon ions with  $Z = 4$  and  $Z = 5$  is given as

$$\langle E \rangle_{\mu, Z=4} = 1.72 E_{\text{cr}}, \quad (16a)$$

$$\langle E \rangle_{\mu, Z=5} = 3.36 E_{\text{cr}}, \quad (16b)$$

thus surpassing (in terms of quantum mechanical average) the Schwinger critical field strength.

The HERCULES laser [49] (still) sets the standard for the highest achievable laser intensities to date, with a peak intensity of about  $2 \times 10^{22} \text{ W cm}^{-2}$ . In the future, such facilities are supposed to reach intensities in the range  $10^{23} \dots 10^{24} \text{ W cm}^{-2}$ . An intensity of  $10^{24} \text{ W cm}^{-2}$  corresponds to an electric field strength of

$$E_L = 2.74 \times 10^{15} \frac{\text{V}}{\text{m}}, \quad (17)$$

which is surpassed in the muonic ( $1 \leq Z \leq 5$ ) as well as medium- $Z$  and high- $Z$  bound quantum electrodynamic

(QED) systems (with  $Z \geq 14$ , see Fig. 3). It is thus evident that bound muonic system offer a competing alternative to the exploration of the strong-field QED regime, complementary to strong laser systems [55].

One might argue that the time average of the oscillating laser fields is zero, as much as the spatial (vector) average of the electric field (vector), taken over the spherically symmetric  $S$  wave function, vanishes. However, the exploration of the strong-field domain of electrodynamics is not precluded by the oscillating or spherically symmetric nature of the fields. One easily estimates that the (fluctuating) electric fields “inside” the proton, given the fact that the three valence quarks cannot be further apart than 0.8 fm, are of order  $E_p \sim 10^{21} \frac{\text{V}}{\text{m}}$  and thus exceed the Schwinger critical field strength  $E_{\text{cr}}$  of about  $E_{\text{cr}} = 1.32 \times 10^{18} \frac{\text{V}}{\text{m}}$  by three orders of magnitude. Conceivable corrections to the muonic hydrogen spectrum due to the high field strengths have been discussed in Refs. [56–58]. Just to avoid a misunderstanding, we should clarify that the recently discussed hypothesis of nonperturbative lepton pairs inside the proton [56–58] certainly does not imply the production of such pairs from the vacuum inside the nucleus; the vacuum is known to “spark” only if the critical field strength is maintained over a sufficiently large space-time interval which is absent in muonic hydrogen. The hypothesis discussed in Refs. [56–58] merely implies that the highly nonperturbative nature of strong interactions (quantum chromodynamics) inside the proton, which involves electrically charged constituent as well as sea quarks, might lead to effective lepton-proton interactions which have so far been overlooked in theoretical treatments (see Refs. [56–58] and Appendix B).

Finally, a remark on the relationship of the light muonic systems and the strong electric fields to the “classical” strong-field systems (highly charged ions) is in order. In these latter systems, the (initially positive-energy)  $1S$  level can be shown to approach the negative continuum, effectively “sparking” the vacuum [59, 60]. A single proton of course is unable to create such an effect, but the proximity of the bound muon to the proton (nucleus) generates the extreme fields and the corresponding quantum mechanical expectation values which contribute to the interest in muonic bound systems.

#### IV. NON-RESONANT EFFECTS AND TRANSITION FREQUENCIES

Discrepancies of Lamb shift experiments and theory have been explored for a long time. For example, a rather well-known accurate Lamb shift experiment in helium [61] has long been in disagreement with theory (the discrepancy has been resolved in Refs. [62, 63]). A measurement of the  $^4\text{He}$  nuclear radius using muonic helium ions is currently in progress [64]. In many cases, nuclear radius determinations using electronic and muonic bound systems complement each other [13]. One may add that



additional experiments on electronic helium ions (as opposed to muonic helium ions) would be able to shed additional light on the “generalized” proton radius puzzle, or “nuclear size effect puzzle”, because they would enable us to compare the “electronically measured” radius of  $^4\text{He}$  with the “muonically measured” radius; a corresponding experimental setup has recently been proposed [65]. In particular, it would be rather interesting to compare the “anisotropy method” used in Refs. [61, 62] with other spectroscopic techniques.

Historical developments encourage us to search for additional conceivable explanations of the proton radius puzzle in systematic effects which may not have been fully appreciated in even the most carefully planned experiments. One such set of corrections is given by so-called off-resonant corrections to frequency measurements. In Ref. [66], it has been stressed that an accurate understanding of the line shape of quantum transitions to neighboring levels can lead to surprising phenomena such as prevention of fluorescence; for precision experiments, this finding highlights the necessity of including a good line-shape model. Because the non-resonant corrections to the line shape involve mixed products of dipole operators connecting the resonant and off-resonant levels, these effects are also referred to as “cross-damping” terms in quantum optics [67, 68] [see also Eq. (9) of Ref. [69]]. In Sec. III of Ref. [69] [see the text after Eq. (15) *ibid.*], the authors investigate off-resonant effects in differential as opposed to angular-averaged cross sections. [Quantum interference effects can be excluded as an explanation of the proton radius discrepancy in muonic systems \[70\], mainly because the proton radius discrepancy, converted to frequency units, is much larger than the natural linewidth of the transitions in the muonic systems. However, the situation is different for atomic hydrogen, where spectral lines have to be split to much higher relative accuracy.](#) In order to gauge possible concomitant systematic shifts of the accurately measured frequencies, especially those involving highly excited states of (atomic) hydrogen and deuterium, improved measurements of hydrogen  $2S$ - $nP$  lines are currently being pursued [71], while an improved measurement of the “classic”  $2S$ - $2P_{1/2}$  Lamb shift is also planned [72]. Both of these experiments have the potential of clarifying the “electronic hydrogen” side of the proton radius puzzle.

In order to understand the importance of the nonresonant terms, and see if they can potentially contribute to the explanation of the proton radius puzzle, let us recall that a typical nonresonant energy shift due to neighboring levels, still displaced by an energy shift  $\Delta E_n$  commensurate with a change in the principal quantum number, is [69, 73]

$$\delta E = \frac{(\hbar\Gamma)^2}{\Delta E_n} \sim \alpha_{\text{QED}}^8 m_e c^2, \quad (18)$$

where  $\Gamma$  is the decay width of the reference state and the term after the “ $\sim$ ” sign is a parametric estimate according to the  $Z\alpha_{\text{QED}}$ -expansion [4]. The shift (18), which ac-

cording to Low [73] defines the ultimate limit to which energy levels can be resolved in spectroscopic experiments, is too small to explain the proton radius puzzle (we have  $\hbar\Gamma \sim \alpha_{\text{QED}}^5 m_e c^2$ , while  $\Delta E_n \sim \alpha_{\text{QED}}^2 m_e c^2$  for a transition with a change in the principal quantum number). By contrast, in differential cross sections, the shift due to neighboring levels removed only by the fine-structure is proportional to [69]

$$\delta E = \frac{(\hbar\Gamma)^2}{\Delta E_{\text{fs}}} \sim \alpha_{\text{QED}}^6 m_e c^2, \quad (19)$$

where  $\Delta E_{\text{fs}} \sim \alpha_{\text{QED}}^4 m_e c^2$  is of the order of a typical fine-structure interval. According to Eqs. (9) and (12) of Ref. [69], there is an additional prefactor 1/2 to consider for the shift of the center of the half-maximum values of the resonance curve, while this prefactor is 1/4 for the Lorentzian maximum itself. The presence of this additional prefactor has no effect on the phenomenological significance of the estimates to be discussed in the following. The shift given in Eq. (19) is of sufficient magnitude to explain the muonic hydrogen discrepancy.

Let us perform some order-of-magnitude estimate to explore the possibility of explaining the proton radius puzzle on the basis of non-resonant corrections. The electron Compton wavelength is  $\lambda_C = \hbar/(m_e c) = 386.159 \text{ fm}$ . The ratio of  $\lambda_C$  to the proton radius, which we assume to be given by  $r_p \approx 0.88 \text{ fm}$ , is given as

$$\xi = \frac{r_p}{\lambda_C} = 2.27 \times 10^{-3}. \quad (20)$$

According to Eq. (51) of Ref. [74] (see also Table 10 of Ref. [10]), the leading-order finite-size effect for the  $2S$  state is as follows (non-recoil limit),

$$E_{FS} = \frac{1}{12} (Z\alpha)^4 m_e c^2 \xi^2 \approx 150 \text{ kHz}. \quad (21)$$

We defined the “proton puzzle prefactor”  $\chi_{PP}$  as

$$\chi_{PP} = \frac{0.88^2 - 0.84^2}{0.88^2} = 0.089, \quad (22)$$

leading to a “proton puzzle energy shift”  $E_{PP}$  for the  $2S$  state of

$$E_{PP} = \chi_P E_{FS} \approx 13 \text{ kHz}. \quad (23)$$

We aim to investigate the possible presence of significant off-resonant corrections to the  $2S$ - $4P_{1/2}$  and  $2S$ - $4P_{3/2}$  frequencies [75], as well as  $2S$ - $8D_{3/2}$  and  $2S$ - $8D_{5/2}$  frequencies [76], and  $2S$ - $12D$  transitions [77]. To this end, we first recall that the fine-structure energy difference, for  $P$  and  $D$  states in hydrogen, is

$$\mathcal{F}_{nP} = E_{nP_{3/2}} - E_{nP_{1/2}} = \chi_{\mathcal{F}P} \frac{(Z\alpha)^4 m_e c^2}{n^3}, \quad (24a)$$

$$\mathcal{F}_{nD} = E_{nD_{5/2}} - E_{nD_{3/2}} = \chi_{\mathcal{F}D} \frac{(Z\alpha)^4 m_e c^2}{n^3}, \quad (24b)$$

$$\chi_{\mathcal{F}P} = \frac{1}{4}, \quad \chi_{\mathcal{F}D} = \frac{1}{12}. \quad (24c)$$

According to p. 266 of Ref. [4], the one-photon decay width of  $nP$  and  $nD$  states can be estimated as (independent of the total angular momentum)

$$\Gamma_{nP} \approx \chi_{\Gamma P} \frac{\alpha (Z\alpha)^4 m_e c^2}{\hbar n^3}, \quad \chi_{\Gamma P} = 0.311, \quad (25a)$$

$$\Gamma_{nD} \approx \chi_{\Gamma D} \frac{\alpha (Z\alpha)^4 m_e c^2}{\hbar n^3}, \quad \chi_{\Gamma D} = 0.107. \quad (25b)$$

We now focus on a potential nonresonant correction to the transition frequencies, due to neighboring fine-structure levels. This choice is motivated in part by a remark in the text in the right-hand column of the second page of Ref. [76], where it is confirmed that neighboring hyperfine structure levels are taken into account in the line-shape model used in Ref. [76] (but those levels displaced by the fine structure apparently are not taken into account).

According to Ref. [69], in an angle-differential cross section, the off-resonant shift due to neighboring fine-structure levels can be estimated as follows. For a  $2S$ - $nP$  transition,

$$E_{OR} = \frac{(\hbar\Gamma)_n^2}{\mathcal{F}_n} = \frac{\chi_{\Gamma}^2}{\chi_{\mathcal{F}}} \frac{\alpha^2 (Z\alpha)^4 m_e c^2}{n^3}, \quad (26)$$

where one has to replace the prefactors as  $\chi_{\Gamma} \rightarrow \chi_{\Gamma P,D}$  and  $\chi_{\mathcal{F}} \rightarrow \chi_{\mathcal{F} P,D}$ , respectively, according to the estimates given in Eqs. (24) and (25).

It is interesting to investigate the ratio of the proton size puzzle energy shift to the natural linewidth as a measure of how precisely the line has to be split in order to resolve the proton size puzzle. It is given as follows ( $2S$ - $nP$  transitions),

$$R_P = \frac{E_{PP}}{\hbar\Gamma_{nP}} = \frac{n^3 \chi_{PP} \xi^2}{12 \alpha \chi_{\Gamma P}} = 1.68 \times 10^{-5} n^3. \quad (27)$$

Example values For  $2S$ - $nP$  are  $R_P(n=4) = 0.0011$ ,  $R_P(n=8) = 0.008$ , and  $R_P(n=12) = 0.029$ . So, in order to resolve the proton size puzzle based on the  $2S$ - $4P$  transition, one has to understand the line width to better than 1 part in 1000. The work [75] reaches an accuracy close to this limit: The experimental accuracy for the  $2S$ - $4P$  transitions is on the order of  $\sim 12$  kHz, to be compared to a natural line width of  $\sim 13$  MHz. The ratio  $R_P$  becomes significantly more favorable for transitions to higher excited  $P$  states.

The corresponding estimate for  $2S$ - $nD$  transitions is

$$R_D = \frac{E_{PP}}{\hbar\Gamma_{nD}} = \frac{n^3 \chi_{PP} \xi^2}{12 \alpha \chi_{\Gamma D}} = 4.86 \times 10^{-5} n^3. \quad (28)$$

For  $2S$ - $nD$  transitions with  $n=4, 8, 12$ , we have  $R_D(n=4) = 0.0031$ ,  $R_D(n=8) = 0.025$ , and  $R_D(n=12) = 0.084$ . It means that in order to resolve the proton size puzzle based on the  $2S$ - $12D$  transition [77], one has to understand the line width only to (roughly) 1 part in 12.

Another interesting quantity is the ratio of the off-resonant terms to the natural linewidth. It measures how

accurately the natural line width has to be split in order to see the off-resonant effects. For  $2S$ - $nP$  transitions and  $2S$ - $nD$  transitions, it is given by

$$S_P = \frac{E_{OR}}{\hbar\Gamma_{nP}} = \frac{\alpha \chi_{\Gamma P}}{\chi_{\mathcal{F} D}} \approx \frac{1}{110}, \quad (29a)$$

$$S_D = \frac{E_{OR}}{\hbar\Gamma_{nD}} = \frac{\alpha \chi_{\Gamma D}}{\chi_{\mathcal{F} D}} \approx \frac{1}{106}, \quad (29b)$$

independent of  $n$ . It is also very important to compare the “proton size puzzle energy shift” to the off-resonant shift. It is given by ( $2S$ - $nP$  transitions)

$$T_P = \frac{E_{PP}}{E_{OR}} = \frac{R_P}{S_P} = \frac{n^3 \chi_{PP} \chi_{\mathcal{F} P} \xi^2}{12 \alpha^2 \chi_{\Gamma P}} = 1.85 \times 10^{-3} n^3. \quad (30)$$

For the  $2S$ - $4P$  transition, one has  $T_P(n=4) = 0.118$ , implying that the off-resonant, cross-damping shift due to neighboring fine-structure levels is roughly ten times larger than the “proton size puzzle energy shift” of the  $2S$  level. We conclude that, unless one uses an appropriate  $4\pi$  detector to eliminate the nonresonant terms, one has to understand the line shape of the  $2S$ - $4P$  transition extremely well in order to resolve proton radius puzzle based on this transition. From a complementary viewpoint, the line shape of the  $2S$ - $4P$  transition could be an excellent tool for studying the nonresonant cross-damping terms.

For  $2S$ - $nD$  transitions, we have

$$T_D = \frac{E_{PP}}{E_{OR}} = \frac{R_D}{S_D} = \frac{n^3 \chi_{PP} \chi_{\mathcal{F} D} \xi^2}{12 \alpha^2 \chi_{\Gamma D}} = 5.16 \times 10^{-3} n^3. \quad (31)$$

Examples are  $T_D(n=8) = 2.64$ , and  $T_D(n=12) = 8.92$ . For the  $2S$ - $8D$  transitions and  $2S$ - $12D$  transitions studied in Refs. [76] and [77], respectively, this means that the estimated ratio of the proton size puzzle energy shift to the off-resonant contribution is larger than unity. One could thus tentatively conclude that the inclusion of any conceivable nonresonant corrections is not likely to shift the experimental results reported in Refs. [76] and [77] on a level commensurate with the proton radius puzzle energy shift.

In summary, our estimates would suggest that  $2S$ - $nD$  transitions to highly excited  $D$  states provide for the most favorable “signal-to-noise” ratio  $E_{PP}/E_{OR}$  [ratio of proton size puzzle energy shift to the off-resonant energy shift, with  $T_D(n=12) = 8.92$ ]. In view of  $R_D(n=12) = 0.084$ , the proton puzzle energy shift enters at about 1/12 of the natural line width [77] for  $n=12$ . Because  $S_D \approx 1/106$ , the off-resonant terms are suppressed by about two orders of magnitude in relation to the natural linewidth, which is smaller than the proton radius puzzle energy shift by roughly another order of magnitude. An inspection of Fig. 1 of Ref. [78] (see also Fig. 1 of Ref. [79]) would indicate that the  $2S$ - $8D$  and  $2S$ - $12D$  transitions are consistent with a proton radius, derived from hydrogen experiments, which is significantly larger than the muonic hydrogen result. A least-squares analysis of all accurately measured hydrogen transitions yields

the proton radius  $r_p = 0.8802(80)$  fm (see Table XLV of Ref. [80]). For comparison, we have exclusively taken the data from the  $2S-8D$  and  $2S-12D$  transitions reported in Refs. [76, 77], together with the latest  $1S-2S$  result [81], and current theory as summarized in Refs. [74, 80], and calculated a naive statistical average of the proton “radii” derived from  $2S-8D$  and  $2S-12D$  transitions (disregarding the covariances among the data which otherwise leads to a much more accurate value for the proton radius [3]). With this approach, the result from  $2S-8D$  and  $2S-12D$  transitions alone is  $r_p = 0.873(17)$  fm, still larger than the muonic hydrogen value by  $2\sigma$ . While the reconsideration of cross-damping terms for hydrogen transitions would be very helpful in clarifying a conceivable contribution to the solution of the proton size puzzle, our estimates suggest that it would be very surprising if the proton size puzzle were to find a full explanation based on the cross-damping terms alone. The off-resonant terms seem to be most effectively suppressed in transitions to highly excited  $D$  states.

## V. CONCLUSIONS

In this paper, we explore the remaining options for the explanation of the persistent proton radius discrepancy [1, 2]. Specifically, in Sec. II, we supplement previous attempts to find an explanation for the proton radius puzzle based on “subversive” virtual particles; all of these appear to require fine-tuning of the coupling constants and no compelling set of quantum numbers has as yet been found for the virtual particle which could potentially explain the discrepancy of theory and experiment in (muonic) hydrogen within the limits set by other precision experiments such as the electron and muon  $g$  factors. Virtual particle explanations appear to be disfavored at the current stage, and other models depend on rather drastic hypotheses such as symmetry breaking terms which affect only the muon sector of the Standard Model (but not electrons or positrons). Here, we supplement the discussions on virtual particles by a calculation of the effective potential describing the leading correction to the Coulomb interaction due to axion-photon conversion in the (strong) magnetic fields used in the muonic hydrogen experiments [1, 2].

In Sec. III, we continue to explore the typical electric fields in a low- $Z$  bound muonic system. These fields are seen to be commensurate with, or even exceed the Schwinger critical field strength. Because of the lack of electron screening, the one-muon ions can be interpreted as the most sensitive probes of high-field physics to date. The hypothesis of nonperturbative lepton pairs inside the proton and their conceivable influence on electron-proton and muon-proton interactions (see Refs. [56–58]) is based on the interplay of nonperturbative quantum chromodynamics with quantum electrodynamics (see Appendix B). A breakdown of perturbative quantum electrodynamics is not necessary for the existence of the conjectured ef-

fect [58]. Muon-proton scattering experiments will be an important cornerstone in the further clarification of the electron-muon universality in lepton-proton interaction (MUSE collaboration, see Ref. [82]).

Finally, in Sec. IV, the role of nonresonant line shifts in differential as opposed to total cross sections is mentioned. Two ongoing experimental efforts [71, 72] share the aim of analyzing the process-dependent line shifts [73] further. Transitions to highly excited  $D$  states ( $2S-nD$  transitions) in hydrogen are identified in terms of favorable parameters for the suppression of nonresonant correction terms (cross-damping terms), which otherwise could account for hitherto unexplored systematic effects in atomic hydrogen experiments. For the muonic hydrogen experiments, in contrast to the experiments on ordinary hydrogen, it is not necessary to “split” the resonance line in order to make the proton radius puzzle manifest; the discrepancy is much larger than the width of the resonance line itself (see Fig. 5 of Ref. [1]).

The binding field strengths in muonic ions exceed those achievable in current and projected high-power laser systems. The benefit of the low- $Z$  muonic ions produced in the high-intensity muon beams at the Paul-Scherrer-Institute (PSI) lies in the “clean” environment provided by the one-muon ions, where all other bound electrons have been stripped and the interaction of the muon and the nucleus can be investigated spectroscopically to high accuracy. From a theoretical point of view, it appears to be hard to shed any further light on the proton radius puzzle without significant further stimulation from additional experimental spectroscopic or scattering data.

## Acknowledgments

Helpful conversation with I. Nándori and M. M. Bush are gratefully acknowledged. The author is grateful to the Mainz Institute for Theoretical Physics (MITP) for its hospitality and its partial support during the completion of this work. This research has been supported by the National Science Foundation (Grants PHY-1068547 and PHY-1403973).

## Appendix A: Heisenberg–Euler Lagrangian and Variational Calculus

In many cases, the leading perturbation to the Coulomb potential due to a “new” interaction can be obtained by variational calculus, and we shall illustrate the procedure here, on the basis of the Wichmann–Kroll correction to the Coulomb potential. The Maxwell Lagrangian with the Heisenberg–Euler Lagrangian reads as



(we switch to natural units with  $\hbar = c = \epsilon_0 = 1$ )

$$\mathcal{L} = \frac{1}{2} (\vec{E}^2 - \vec{B}^2) + \frac{2\alpha_{\text{QED}}^2}{45m^4} (\vec{E}^2 - \vec{B}^2)^2 + \frac{14\alpha_{\text{QED}}^2}{45m^4} (\vec{E} \cdot \vec{B})^2. \quad (\text{A1})$$

If  $\vec{E}$  is given by the gradient of a Coulomb field and the magnetic field vanishes ( $\vec{B} = \vec{0}$ ), then  $\mathcal{L}$  is redefined to the expression

$$\mathcal{L} = \frac{1}{2} (\vec{\nabla}\Phi)^2 + \frac{2\alpha_{\text{QED}}^2}{45m^4} (\vec{\nabla}\Phi)^4 - \rho\Phi, \quad (\text{A2})$$

where we add the source term. In view of the relations

$$\frac{\partial\mathcal{L}}{\partial\vec{\nabla}\Phi} = \vec{\nabla}\Phi + \frac{8\alpha_{\text{QED}}^2}{45m^4} \vec{\nabla}\Phi (\vec{\nabla}\Phi)^2, \quad \frac{\partial\mathcal{L}}{\partial\Phi} = -\rho, \quad (\text{A3})$$

the variational equation  $\vec{\nabla} \cdot \frac{\partial\mathcal{L}}{\partial\vec{\nabla}\Phi} = \frac{\partial\mathcal{L}}{\partial\Phi}$  becomes

$$\vec{\nabla}^2\Phi + \frac{8\alpha_{\text{QED}}^2}{45m^4} \left( \vec{\nabla}^2\Phi (\vec{\nabla}\Phi)^2 + \vec{\nabla}\Phi \cdot \vec{\nabla} (\vec{\nabla}\Phi)^2 \right) = -\rho, \quad (\text{A4})$$

which can be reformulated as

$$\vec{\nabla}^2\Phi + \frac{8\alpha_{\text{QED}}^2}{45m^4} \left( \partial_r + \frac{2}{r} \right) (\partial_r\Phi)^3 = -\rho. \quad (\text{A5})$$

where we assume that  $\Phi$  is radially symmetric. We set  $\Phi = \Phi_C + \Xi$  where  $\Phi_C$  is the Coulomb potential and  $\Xi$  is a quantum correction. The charge density of the nucleus and the Coulomb potential are given by

$$\rho(\vec{r}) = Z|e|\delta^{(3)}(\vec{r}), \quad \Phi_C(\vec{r}) = \frac{Z|e|}{4\pi r}, \quad (\text{A6})$$

where  $\vec{\nabla}^2\Phi_C(\vec{r}) = -\rho(\vec{r})$ , so that, to first order in  $\Xi$ ,

$$\left( \partial_r^2 + \frac{2}{r} \partial_r \right) \Xi + \frac{8\alpha_{\text{QED}}^2}{45m^4} \left( \partial_r + \frac{2}{r} \right) (\partial_r\Phi_C)^3 = 0. \quad (\text{A7})$$

It is straightforward to observe that Eq. (A7) is solved by a potential proportional to  $r^{-5}$ ,

$$\Phi = \Phi_C + \Xi = \frac{Z|e|}{4\pi r} \left( 1 - \frac{2}{225} \frac{\alpha_{\text{QED}}}{\pi} \frac{(Z\alpha_{\text{QED}})^2}{(mr)^4} \right), \quad (\text{A8})$$

This is equal to the “long-distance” tail of the Wichmann-Kroll potential [83, 84], which is relevant to a distance range  $r \sim a_0$ , where  $a_0$  is the Bohr radius; we here confirm the result given in Appendix III of Ref. [84].

A few remarks are in order. Matrix elements of a term of order  $(\alpha_{\text{QED}}/\pi) (Z\alpha_{\text{QED}})^3/(m^4 r^5)$  [see Eq. (A8)] generate an energy shift proportional to  $\alpha_{\text{QED}} (Z\alpha_{\text{QED}})^8 m$  in hydrogenlike systems. By contrast, the “leading term” in the Wichmann-Kroll potential is otherwise proportional to a Dirac- $\delta$  function and generates an energy

shift of the order of  $\alpha_{\text{QED}} (Z\alpha_{\text{QED}})^6 m$ . The latter term is given by the high-energy (short-distance) regime not covered by our variational ansatz. Namely, the atomic nucleus, the Coulomb potential and its derivative, the Coulomb field, vary considerably on the length scale of an electron Compton wavelength, which exceeds the “operational parameters” of the Heisenberg-Euler Lagrangian, so the result (A8) cannot be used for distances closer than an electron Compton wavelength, i.e., it fails in the immediate vicinity of the nucleus.

One might wonder why the functional form of the long-distance tail ( $1/r^5$  for the Wichmann-Kroll potential) is different from the corresponding term for the Uehling potential, which decays exponentially at large distances (see [12] and references therein). The answer to this question is that the Wichmann-Kroll potential, which is generated by Feynman diagrams with at least four electromagnetic interaction terms inside the loop, can be related to the Heisenberg-Euler effective Lagrangian, which is valid for the long-distance tail of the potential, while the corresponding term, for the Uehling potential (with only two electromagnetic interaction terms inside the loop) would otherwise generate a term proportional to  $\vec{E}^2$  which is absorbed in the  $Z_3$  renormalization of the electromagnetic charge [85]. Hence, the tail of the Uehling potential decays exponentially, akin to a Yukawa potential, with a range of the potential being proportional to the electron Compton wavelength (Sec. 2.4 of Ref. [12]).

After these intermediate considerations, we may proceed to apply our variational ansatz to a calculation of interest in the context of the subject matter of the current investigation. Namely, for a nonvanishing vacuum expectation value  $\langle\phi\rangle \neq 0$  of the axion-like particle as a dark matter candidate, the Lagrangian [39, 40]

$$\mathcal{L}_A = \frac{1}{2} (\vec{E}^2 - \vec{B}^2) + g \langle\phi\rangle \vec{E} \cdot \vec{B} \quad (\text{A9})$$

is exact up to possible QED or axion loop corrections; in contrast to the Heisenberg-Euler Lagrangian, it is not the result of “integrating out” the fermionic degrees of freedom which limits the “operational parameters” of the Lagrangian (A1). Hence, we are not at risk of exceeding the “operational parameters of the variational ansatz” when we use the axion background Lagrangian (A9) to calculate a possible correction to the Coulomb potential due to dark matter physics. If  $\vec{E} = -\vec{\nabla}\Phi$  is generated by a (possibly distorted) Coulomb field and  $\vec{B}$  is the (possibly inhomogeneous) external magnetic field, then the Lagrange density  $\mathcal{L}_A$  is redefined to read (adding the source term  $\rho\Phi$ )

$$\mathcal{L}_A = \frac{1}{2} (\vec{\nabla}\Phi)^2 - g \langle\phi\rangle \vec{B} \cdot \vec{\nabla}\Phi - \rho\Phi. \quad (\text{A10})$$

The variational equation

$$\vec{\nabla} \cdot \frac{\partial\mathcal{L}_A}{\partial\vec{\nabla}\Phi} = \frac{\partial\mathcal{L}_A}{\partial\Phi} \quad (\text{A11})$$

becomes

$$\vec{\nabla}^2 \Phi - g \langle \phi \rangle \vec{\nabla} \cdot \vec{B} = -\rho. \quad (\text{A12})$$

In the absence of magnetic monopoles, the leading correction to the Coulomb potential mediated by the axion vacuum expectation value thus vanishes, even for very strong and inhomogeneous external magnetic fields  $\vec{B}$ .

One more remark is in order. The direct coupling of the fermion to the axion [29] is of the derivative form  $\mathcal{L}_{Aff} = (C_f/(2f_A)) \bar{\psi}_f \gamma^\mu \gamma_5 \psi_f \partial_\mu \phi$ , where  $C_f$  is a model-dependent constant. The Yukawa coupling is  $g_{Aff} = C_f m_f/f_A$  and the “fine-structure constant” is  $g_{Aff}^2/(4\pi)$ ; energy loss arguments from the SN1987A supernova typically give bounds in the range  $g_{Aff}^2/(4\pi) \sim 10^{-21}$  (see Refs. [86, 87]). This implies that a single axion exchange, or an axion interaction insertion (e.g., into the fermion line of a vacuum polarization diagram) suffers from a suppression factor on the order of  $g_{Aff}^2/(4\pi) \sim 10^{-21}$  and is thus suppressed with respect to the corresponding photon exchange diagram (coupling parameter  $\alpha_{\text{QED}}$ ) by roughly 18 orders of magnitude. The fermion-axion coupling thus is too small to explain the proton radius puzzle. Axion-mediated effects as well as weak interactions [88] can thus also be excluded as possible explanations for the proton radius puzzle.

## Appendix B: Strong Fields in the Proton, Interplay of QED and QCD

The presence of a very small fraction of “light sea fermions”, conceivably due to a nonperturbative mechanism, inside the proton, has recently been mentioned in Refs. [56, 57]. One might counter-argue that the QED running coupling constant, at distances commensurate with the proton radius, still is small against unity, and that this precludes a nonperturbative mechanism leading to sea fermions inside the proton. In Sec. III of Ref. [56], it is argued that the highly nonperturbative quantum chromodynamic (QCD) nature of a hypothetical “electrically neutral” proton receives a “correction” due to the electroweak interactions, as they are “switched back on”, and that, due to the highly nonlinear nonperturbative nature of QCD, this reshaping can be much larger than the electromagnetic perturbation itself.

Alternatively, one might argue that the fundamentally nonperturbative nature of the QCD interaction inside the proton might leave room for effects that cannot be described by dispersion relations and perturbation theory alone. Namely, due to the nonperturbative nature of QCD, the three valence quarks of the proton are supplemented, at any given time, by a large number of “virtual” sea quarks which emerge from the vacuum due to quantum corrections to the gluon exchange [89]. The sea quarks, as much as the valence quarks, are electrically charged, off of their mass shell, and may exchange photons. The propagator of these photons, in turn, receives

a correction due to vacuum polarization; hence, at any given time, the proton wave function has a nonvanishing electron-positron content due to the light fermionic vacuum bubbles. This is a persistent phenomenon because the quarks inside the proton are always highly “virtual” (off mass shell) in view of their strong (mutual) interactions [58].

In Ref. [58], the lepton pair content has recently been estimated based on a (perturbative) calculation of the electron-positron vacuum polarization insertion into the radiative correction to a constituent quark’s vector and axial vector current matrix elements. According to Ref. [56], the virtual annihilation channel in positronium,

$$\delta H = \frac{\pi \alpha_{\text{QED}}}{2m_e^2} (3 + \vec{\sigma}_+ \cdot \vec{\sigma}_-) \delta^3(r), \quad (\text{B1})$$

corresponds to an effective Hamiltonian for electron-proton interactions of the form

$$H_{\text{ann}} = \epsilon_p \frac{3\pi \alpha_{\text{QED}}}{2m_e^2} \delta^3(r), \quad (\text{B2})$$

where  $\epsilon_p$  measures the electron-positron pair content inside the proton and a value of  $\epsilon_p = 2.1 \times 10^{-7}$  is found to be sufficient to explain the proton radius puzzle. Near Eq. (22) of Ref. [58], it is argued that instead of Eq. (B1), one should rather consider the Hamiltonian

$$\delta H = \frac{\pi \alpha_{\text{QED}}}{2m_q^2} (3 + \vec{\sigma}_+ \cdot \vec{\sigma}_-) \delta^3(r), \quad (\text{B3})$$

where  $m_q$  is a quark mass. According to Ref. [58], an appropriate choice is  $m_q \approx 600 m_e$  (constituent value of one third of the mass of a proton). Comparing Eqs. (B1), (B2) and (B3), one is led to the identification  $\epsilon_p \sim m_e^2/m_q^2 \approx 2.8 \times 10^{-6}$  which is “too large” to explain the proton radius puzzle. An estimate of the lepton pair content of the proton, based on electron-positron vacuum polarization insertions into the radiative correction to a constituent quark’s vector and axial vector current, likewise leads to estimates for  $\epsilon_p$  which are “too large” to explain the discrepancy. According to Eqs. (13) and (21) of Ref. [58], and estimate based on matrix elements of the current leads to values in the range

$$\epsilon_p \sim 10 \left( \frac{\alpha_{\text{QED}}}{\pi} \right)^2 \sim 10^{-5} \gg 10^{-7}. \quad (\text{B4})$$

Conversely, if one starts from Eq. (B3) instead of (B1), arguing that the effective mass in the virtual annihilation diagram should be the quark mass, and *additionally* invokes the suppression factor  $\epsilon_p$  [see the text following Eq. (22) of Ref. [58]], then the resulting effect in muonic hydrogen becomes negligible on the level of the proton radius discrepancy. Guidance for the exploration of the conjectured sea lepton effect in future experiments is given by the discussion surrounding Eq. (23) of Ref. [58], where the functional dependence on the charge and mass numbers of the nucleus is discussed.

Nuclear structure corrections (nuclear polarizability corrections) are usually taken into account with the use of dispersion relations [90]. This is certainly a valid approach for genuine excitations of the valence quarks into excited states. However, the light sea fermions are generated by a QED correction to a nonperturbative process, namely, a correction to the nonperturbative QCD interaction inside the proton; the latter gives rise to the ubiquitous sea quarks. Dispersion relations (Cutkosky rules) are available for the treatment of the genuine excitations

of the proton into its own excited states, but it is unclear if the use of dispersion relations could capture the effect of the sea fermions. Because the sea quark interaction is nonperturbative and the light fermion vacuum bubbles are inserted into the photon exchange among the (nonperturbative) sea quarks, one does not know where to cut the nonperturbative diagram, and the dispersion relation is not available. For further details, we refer to Refs. [56–58].

- 
- [1] R. Pohl *et al.*, *Nature* (London) **466**, 213 (2010).
  - [2] A. Antognini *et al.*, *Science* **339**, 417 (2013).
  - [3] U. D. Jentschura, S. Kotochigova, E.-O. Le Bigot, P. J. Mohr, and B. N. Taylor, *Phys. Rev. Lett.* **95**, 163003 (2005).
  - [4] H. A. Bethe and E. E. Salpeter, *Quantum Mechanics of One- and Two-Electron Atoms* (Springer, Berlin, 1957).
  - [5] S. J. Brodsky and P. J. Mohr, in *Structure and Collisions of Ions and Atoms*, edited by I. A. Sellin (Springer, Berlin, 1978), pp. 3–67.
  - [6] H. F. Beyer, H.-J. Kluge, and V. P. Shevelko, *X-Ray Radiation of Highly Charged Ions* (Springer, Berlin-Heidelberg, 1997).
  - [7] G. Soff, T. Beier, M. Greiner, H. Persson, and G. Plunien, *Adv. Quant. Chem.* **30**, 125 (1998).
  - [8] P. J. Mohr, G. Plunien, and G. Soff, *Phys. Rep.* **293**, 227 (1998).
  - [9] G. Soff *et al.*, *Hyp. Int.* **132**, 75 (2001).
  - [10] M. I. Eides, H. Grotch, and V. A. Shelyuto, *Phys. Rep.* **342**, 63 (2001).
  - [11] M. I. Eides, H. Grotch, and V. A. Shelyuto, *Theory of Light Hydrogenic Bound States — Springer Tracts in Modern Physics 222* (Springer, Berlin, Heidelberg, New York, 2007).
  - [12] U. D. Jentschura, *Ann. Phys. (N.Y.)* **326**, 500 (2011).
  - [13] U. D. Jentschura, *Ann. Phys. (N.Y.)* **326**, 516 (2011).
  - [14] A. Antognini *et al.*, *Ann. Phys. (N.Y.)* **331**, 127 (2013).
  - [15] C. E. Carlson and B. C. Rislow, *Phys. Rev. D* **86**, 035013 (2012).
  - [16] B. Batell, D. McKeen, and M. Pospelov, *Phys. Rev. Lett.* **107**, 011803 (2011).
  - [17] L. Camilleri *et al.*, *Phys. Rev. Lett.* **23**, 153 (1969).
  - [18] T. J. Braunstein *et al.*, *Phys. Rev. D* **6**, 106 (1972).
  - [19] A. H. Gomes, V. A. Kosteletzky, and A. J. Vargas, *Phys. Rev. D* **90**, 076009 (2014).
  - [20] A. de Rujula, *Phys. Lett. B* **693**, 555 (2010).
  - [21] R. D. Peccei and H. R. Quinn, *Phys. Rev. Lett.* **38**, 1440 (1977).
  - [22] H. Gies, J. Jaeckel, and A. Ringwald, *Phys. Rev. Lett.* **97**, 140402 (2006).
  - [23] M. Ahlers, H. Gies, J. Jaeckel, and A. Ringwald, *Phys. Rev. D* **75**, 035011 (2007).
  - [24] M. Ahlers, H. Gies, J. Jaeckel, J. Redondo, and A. Ringwald, *Phys. Rev. D* **77**, 095001 (2008).
  - [25] P. Sikivie, *Phys. Rev. Lett.* **51**, 1415 (1983).
  - [26] H. Gies, *J. Phys. A* **41**, 164039 (2008).
  - [27] K. Ehret *et al.*, *Nucl. Instrum. Methods A* **612**, 83 (2009).
  - [28] K. Ehret *et al.*, *Phys. Lett. B* **689**, 149 (2010).
  - [29] J. Beringer *et al.* [Particle Data Group], *Phys. Rev. D* **86**, 010001 (2012).
  - [30] M. Dine, W. Fischler, and M. Srednicki, *Phys. Lett. B* **104**, 199 (1981).
  - [31] A. R. Zhitnitsky, *Sov. J. Nucl. Phys.* **31**, 260 (1980).
  - [32] J. E. Kim, *Phys. Rev. Lett.* **43**, 103 (1979).
  - [33] M. A. Shifman, A. I. Vainshtein, and V. I. Zakharov, *Nucl. Phys. B* **166**, 493 (1980).
  - [34] S. L. Cheng, C. Q. Geng, and W. T. Ni, *Phys. Rev. D* **52**, 3132 (1995).
  - [35] S. Villalba-Chavez and A. di Piazza, *J. High Energy Phys.* **11**, 136 (2013).
  - [36] S. Villalba-Chavez, *Nucl. Phys. B* **881**, 391 (2014).
  - [37] V. B. Berestetskii, E. M. Lifshitz, and L. P. Pitaevskii, *Quantum Electrodynamics, Volume 4 of the Course on Theoretical Physics*, 2 ed. (Pergamon Press, Oxford, UK, 1982).
  - [38] W. E. Caswell and G. P. Lepage, *Phys. Lett. B* **167**, 437 (1986).
  - [39] L. D. Duffy and K. van Bibber, *New J. Phys.* **11**, 105008 (2009).
  - [40] J. Barranco, A. Carrillo Monteverde, and D. Delepine, *J. Phys. Conf. Ser.* **485**, 012035 (2014).
  - [41] I. Beltrami *et al.*, *Nucl. Phys. A* **451**, 679 (1986).
  - [42] R. D. Deslattes, E. G. Kessler, W. C. Sauder, and A. Henins, *Ann. Phys. (N.Y.)* **129**, 378 (1980).
  - [43] W. Ruckstuhl *et al.*, *Nucl. Phys. A* **430**, 685 (1984).
  - [44] E. A. J. M. Offermann *et al.*, *Phys. Rev. C* **44**, 1096 (1991).
  - [45] J.-P. Karr and L. Hilico, *Phys. Rev. Lett.* **109**, 103401 (2012).
  - [46] M. Umair and S. Jonsell, *J. Phys. B* **47**, 175003 (2014).
  - [47] D. C. Ionescu, J. Reinhardt, B. Müller, W. Greiner, and G. Soff, *Phys. Rev. A* **38**, 616 (1988).
  - [48] A. Gumberidze *et al.*, *Phys. Rev. Lett.* **94**, 223001 (2005).
  - [49] I. V. Yanovsky *et al.*, *Opt. Express* **16**, 2109 (2008).
  - [50] F. Sauter, *Z. Phys.* **73**, 742 (1931).
  - [51] F. Sauter, *Z. Phys.* **73**, 547 (1931).
  - [52] W. Heisenberg and H. Euler, *Z. Phys.* **98**, 714 (1936).
  - [53] J. Schwinger, *Phys. Rev.* **82**, 664 (1951).
  - [54] R. A. Swainson and G. W. F. Drake, *J. Phys. A* **24**, 79 (1991).
  - [55] C. H. Keitel, *Contemp. Phys.* **42**, 353 (2001).
  - [56] U. D. Jentschura, *Phys. Rev. A* **88**, 062514 (2013).
  - [57] K. Pachucki and K. Meissner, *Proton charge radius and the perturbative quantum electrodynamics*, e-print arXiv:1405.6582.
  - [58] G. A. Miller, 2015.
  - [59] Y. B. Zel'dovich and V. S. Popov, *Usp. Fiz. Nauk* **105**, 403 (1971), [*Sov. Phys. Usp.* **14**, 673 (1972)].

- [60] J. Rafelski, B. Müller, and W. Greiner, Nucl. Phys. B **68**, 585 (1974).
- [61] A. van Wijngaarden, J. Kwela, and G. W. F. Drake, Phys. Rev. A **43**, 3325 (1991).
- [62] A. van Wijngaarden, F. Holuj, and G. W. F. Drake, Phys. Rev. A **63**, 012505 (2000).
- [63] U. D. Jentschura and G. W. F. Drake, Can. J. Phys. **82**, 103 (2004).
- [64] R. Pohl, private communication (2014).
- [65] M. Herrmann *et al.*, Phys. Rev. A **79**, 052505 (2009).
- [66] D. A. Cardimona, M. G. Raymer, and C. R. Stroud, J. Phys. B **15**, 55 (1982).
- [67] Z. Ficek and S. Swain, J. Mod. Opt. **49**, 3 (2002).
- [68] Z. Ficek and S. Swain, *Quantum Interference and Coherence — Springer Series in Optical Sciences vol. 100* (Springer, Berlin, Heidelberg, New York, to appear in 2005, ISBN: 0-387-22965-5).
- [69] U. D. Jentschura and P. J. Mohr, Can. J. Phys. **80**, 633 (2002).
- [70] P. Amaro *et al.*, *Quantum interference effects in laser spectroscopy of muonic hydrogen, deuterium and helium-3*, e-print arXiv:1506.02734v1 [physics.atom-ph].
- [71] T. Udem, private communication (2014).
- [72] E. Hessels, private communication (2014).
- [73] F. Low, Phys. Rev. **88**, 53 (1952).
- [74] P. J. Mohr, B. N. Taylor, and D. B. Newell, Rev. Mod. Phys. **80**, 633 (2008).
- [75] D. J. Berkeland, E. A. Hinds, and M. G. Boshier, Phys. Rev. Lett. **75**, 2470 (1995).
- [76] B. de Beauvoir *et al.*, Phys. Rev. Lett. **78**, 440 (1997).
- [77] C. Schwob *et al.*, Phys. Rev. Lett. **82**, 4960 (1999), [Erratum Phys. Rev. **86**, 4193 (2001)].
- [78] A. Beyer *et al.*, Ann. Phys. (Berlin) **525**, 671 (2013).
- [79] A. Beyer *et al.*, J. Phys. Conf. Ser. **467**, 012003 (2013).
- [80] P. J. Mohr, B. N. Taylor, and D. B. Newell, Rev. Mod. Phys. **84**, 1527 (2012).
- [81] A. Matveev *et al.*, Phys. Rev. Lett. **110**, 230801 (2013).
- [82] M. Kohl *et al.* [MUSE Collaboration], Eur. Phys. J. Web of Conferences **66**, 06010 (2014).
- [83] E. H. Wichmann and N. M. Kroll, Phys. Rev. **96**, 232 (1954).
- [84] E. H. Wichmann and N. M. Kroll, Phys. Rev. **101**, 843 (1956).
- [85] C. Itzykson and J. B. Zuber, *Quantum Field Theory* (McGraw-Hill, New York, 1980).
- [86] J. A. Grifols, E. Masso, and S. Peris, Mod. Phys. Lett. A **4**, 311 (1989).
- [87] G. G. Raffelt, Phys. Rep. **198**, 1 (1990).
- [88] M. I. Eides, Phys. Rev. A **85**, 034503 (2012).
- [89] C. Gattringer and C. B. Lang, *Quantum Chromodynamics on the Lattice: An Introductory Presentation (Lecture Notes in Physics Vol. 788)* (Springer, Heidelberg, 2009).
- [90] C. E. Carlson, M. Gorchtein, and M. Vanderhaeghen, Phys. Rev. A **89**, 022504 (2014).